Available online at www.sciencedirect.com
ScienceDirect
Journal of Hazardous Materials 140 (2007) 333–339
Journal of Hazardous Materials
www.elsevier.com/locate/jhazmat

Vitrification of copper flotation waste

Alexander Karamanov [a,*], Mirko Aloisi [b], Mario Pelino [b]

[a] *Institute of Physical Chemistry, Bulgarian Academy of Science, G. Bonchev Str. Block 11, 1113 Sofia, Bulgaria*
[b] *Department of Chemistry, Chemical Engineering and Materials, University of L'Aquila, 67040 Monteluco di Roio, L'Aquila, Italy*

Received 26 April 2006; received in revised form 21 August 2006; accepted 9 September 2006
Available online 23 September 2006

Abstract

The vitrification of an hazardous iron-rich waste (W), arising from slag flotation of copper production, was studied. Two glasses, containing 30 wt% W were melted for 30 min at 1400 °C. The first batch, labeled WSZ, was obtained by mixing W, blast furnace slag (S) and zeolite tuff (Z), whereas the second, labeled WG, was prepared by mixing W, glass cullet (G), sand and limestone. The glass frits showed high chemical durability, measured by the TCLP test.

The crystallization of the glasses was evaluated by DTA. The crystal phases formed were identified by XRD resulting to be pyroxene and wollastonite solid solutions, magnetite and hematite. The morphology of the glass–ceramics was observed by optical and scanning electron microscopy. WSZ composition showed a high rate of bulk crystallization and resulted to be suitable for producing glass–ceramics by a short crystallization heat-treatment. WG composition showed a low crystallization rate and good sinterability; glass–ceramics were obtained by sinter-crystallization of the glass frit.

Keywords: Hazardous waste; Glass–ceramics

1. Introduction

Iron-rich glass compositions are industrially produced by re-fused rocks (petrurgy). The development of these materials started after the First World War and today they are considered as a precursor of glass–ceramics [1–4]. The main products are building tiles obtained by pressing or casting, pipes and bends obtained by centrifuging and glass fibers. A typical petrurgical raw material is the basalt rock composition, containing 10–15 wt% iron oxides; it is characterized by high chemical durability and good resistance to abrasion and corrosion.

Due to the high chemical durability of the natural basalts, iron-rich glass and glass–ceramic materials with basalt-like compositions were developed for nuclear waste disposal [5–7]. Recently, materials with very high iron content (up to 20–25 wt%) were obtained by the vitrification of hazardous industrial wastes [8–16], arising from the zinc hydrometallurgy (jarosite and goethite) and by electric arc furnace dusts (EAFD) from the steel production [17–20]. Iron-rich glass–ceramics were also obtained by other industrial streams [21–25].

The iron in the glass structure is present in both Fe^{3+} and Fe^{2+} forms; the Fe^{3+}/Fe^{2+} ratio depends on the melting conditions and the glass compositions [2,6,12,13]. Since in the glass structure Fe_2O_3 is an intermediate oxide and FeO is a modifying the rise of the Fe^{3+}/Fe^{2+} ratio increases the viscosity and improves both the chemical durability and mechanical properties. At high temperature, the iron-rich silicate compositions are characterized by a liquid–liquid immiscibility leading to the formation of an iron-rich liquid phase, which may promote the precipitation of the magnetite spinels during cooling [9,15].

The iron-rich glass–ceramics can also be obtained by the sinter-crystallization technology, which gives the possibility to obtain materials with complicated shapes and good mechanical properties [16], as well as to produce tiling panels with an attractive appearance [11]. When heat-treating iron-rich glass powder above the glass transformation range, the oxidation of Fe^{2+} to yield Fe^{3+} takes place producing variation of the chemical compositions of the surface and sub-surface layers [26,27], influencing the crystallization and leading to hematite formation on the surface [11,12,15].

* Corresponding author at: Department of Chemistry, Chemical Engineering and Materials, University of L'Aquila, 67040 Monteluco di Roio, L'Aquila, Italy. Tel.: +39 0862 434233; fax: +39 0862 434233.
E-mail address: karama@ing.univaq.it (A. Karamanov).

0304-3894/$ – see front matter © 2006 Elsevier B.V. All rights reserved.
doi:10.1016/j.jhazmat.2006.09.040

In this work, the vitrification of an hazardous waste arising from the flotation of copper ores and containing about 70 wt% iron oxides, was studied. Two batches were obtained by mixing 30 wt% of waste with blast furnace slag and zeolite tuff or, alternatively, with glass cullet, sand and limestone.

2. Industrial wastes and raw materials

2.1. Copper flotation waste (W)

Copper is produced by concentrating low-grade ores containing copper sulfide minerals, followed by smelting and electrolytic refining to produce pure copper cathode. The slag, after grinding and flotation, is returned to reverberatory furnaces to recover the remaining copper.

In the present work, the flotation waste from the Samsun Flash Smelting Plant (Turkey) was used. The plant produces about 40,000 metric tonnes of blister copper and about 150,000 metric tonnes of flotation waste per year.

2.2. Blast furnace slag (S)

The blast furnace slag is an inert waste, widely used as raw material in different silicates industries (cement, glass and glass–ceramics production). Depending on the cooling techniques, foamed, pelletized or granulated blast furnace slag are obtained. In the last case, the molten slag is quenched in water, leading to the formation of frit-like particles with 1–5 mm size. In the present study, granulated blast furnace slag from Kardemir Co. Plant (Turkey), located about 150 km from the copper flotation plant was used.

2.3. Zeolite tuff (Z)

Zeolite tuff is widely present in the tertiary sediments of the Çnkırı-Çorum Basin in Turkey. The material is widely used as aggregates and ornamental stone in the building industry. The zeolite tuff deposit is located at 80 km from the copper plant.

2.4. Glass cullet (G)

The glass cullet is a typical additive for the synthesis of glass and glass–ceramics from industrial wastes. Its addition decreases the melting temperature and reduces the melting time. In present study non-colored clean container glass, crushed bellow 2 mm, is used.

3. Experimental

The chemical and the mineralogical compositions of the waste and raw materials were evaluated by XRF (Spectro-Xepos) and XRD (Philips PW1830 and Cu Kα radiation) analyses, respectively. The thermal behavior was studied by DTA–TG analysis (Netzsch STA 409).

Two different batches of 200 g were melted in 200 ml alumina crucibles at 1400 °C for 30 min. The melting was realized in electric furnace and at static air atmosphere. About 100 g batch was put in the crucible before melting, while the other 100 g was added at 1250–1300 °C. Part of the melt was quenched in water to obtain glass frit; the other part was quenched on a cold steel mould.

The chemical durability of the flotation waste and obtained glasses were estimated by the toxicity characterization leaching procedure (TCLP). The dried waste and glass frit (with 0.1–5 mm size) were placed in distillated water and stirred for 24 h at room temperature. The pH of the solution was kept constant to 5 ± 0.2 by addition of 0.5 M acetic acid. The analyses on the liquid extraction phase were carried out by atomic adsorption spectroscopy (Varian Spectra 200).

The crystallization behavior of the glasses was evaluated by DTA using 100–110 mg bulk and powder (<75 μm) samples at 10 °C/min heating rate in air and nitrogen atmosphere. The formed crystalline phases were evaluated by XRD analysis. The degree of crystallinity was estimated by comparing the intensity of the amorphous halo in XRD spectra of the parent glasses with the one of the glass–ceramic [28]; the ratio between the different phases was evaluated by comparing the intensities of the major peaks.

Table 1
Chemical compositions of the used copper flotation waste (W), blast furnace slag (S), zeolite tuff (Z), glass cullet (G) and WG and WSZ glasses (wt%)

	W	S	Z	G	WSZ	WG
SiO_2	24.93 ± 0.04	39.89 ± 0.04	64.32 ± 0.05	71.91 ± 0.05	46.18 ± 0.04	56.56 ± 0.06
Al_2O_3	0.88 ± 0.01	9.32 ± 0.03	12.11 ± 0.03	1.54 ± 0.02	10.44 ± 0.04	3.01 ± 0.02
Fe_2O_3[a]	67.72 ± 0.03	1.15 ± 0.01	0.82 ± 0.01	0.24 ± 0.01	21.58 ± 0.02	19.89 ± 0.02
CaO	0.72 ± 0.01	34.88 ± 0.02	2.49 ± 0.01	10.24 ± 0.01	11.98 ± 0.02	10.83 ± 0.01
MgO	0.43 ± 0.02	8.09 ± 0.04	2.12 ± 0.02	0.89 ± 0.02	3.43 ± 0.03	0.18 ± 0.02
CuO	1.01 ± 0.01	0.88 ± 0.01	–	–	0.32 ± 0.01	0.29 ± 0.01
ZnO	2.82 ± 0.02	–	–	–	0.91 ± 0.01	0.88 ± 0.01
PbO	0.31 ± 0.01	–	–	–	0.11 ± 0.01	0.10 ± 0.01
BaO	0.11 ± 0.01	1.21 ± 0.01	0.09 ± 0.01	–	0.27 ± 0.01	–
MnO	0.89 ± 0.01	2.81 ± 0.01	–	–	0.98 ± 0.01	–
K_2O	0.46 ± 0.01	1.43 ± 0.01	0.82 ± 0.01	0.37 ± 0.01	0.84 ± 0.01	0.19 ± 0.01
Na_2O	–	0.24 ± 0.05	5.62 ± 0.07	15.52 ± 0.12	2.35 ± 0.05	6.88 ± 0.07
SO_3[a]	2.16 ± 0.01	1.35 ± 0.02	0.24 ± 0.01	–	0.09 ± 0.01	0.08 ± 0.01
Others	0.4	0.1	0.6		0.4	0.1

[a] Iron is presented as Fe_2O_3 and sulfur as SO_3.

The crystalline morphology of the glass–ceramic samples was studied by optical and scanning electron microscopes, after polishing the surface followed by 8 s etching with 2 wt% HF.

4. Results and discussion

4.1. Characterization of the wastes and glasses

The chemical compositions are presented in Table 1. The XRD spectra of the flotation waste, blast furnace slag and zeolite tuff are shown in Fig. 1, while the corresponding DTA (solid lines) and TG (trashed lines) traces are presented in Fig. 2.

The chemical composition of the flotation waste, W, contains iron oxide and silica, together with ZnO, CuO and PbO. The XRD spectrum shows mainly magnetite ($FeO{\cdot}Fe_2O_3$) and fayalite ($2FeO{\cdot}SiO_2$), together with some traces of iron and copper sulfides. The DTA shows exo-peaks at 480 and 725 °C with 4.5 wt% rise in the TG signal, related to the oxidation of iron and copper sulfides and an endo-effect at 1355 °C with 3% weight loss due to the release of sulfur oxides. In agreement with the Si–Fe–O phase diagram, melting endo-effects of fayalite and magnetite are observed at 1160 and 1435 °C, respectively [3].

The chemical composition of the slag, S, is mainly constituted by SiO_2 and CaO, together with MgO and MnO. The XRD analysis highlights an amorphous structure. The DTA traces shows a glass-transition point at 710 °C, intensive crystallization exo-peak with maximum at 1005 °C and melting endo-effects in the range 1150–1300 °C. The TG traces shows no significant weight variations.

The composition of the zeolite tuff, Z, is mainly constituted by SiO_2 and Al_2O_3, together with N_2O, CaO and MgO. The XRD analysis corresponds to clinoptilolite ($KNa_2Ca_2(Si_{29}Al_{17})O_{72}{\cdot}24H_2O$). The TG–DTA results show a clear endo-effect at 215 °C, related to a 10% loss of structural water in the interval of 150–350 °C. Another 2% loss is observed in the 650–750 °C interval and is related to the endo-effect at 735 °C. Melting endo-peaks with low intensity are observed in the 1150–1250 °C range. A similar thermal behavior of the clinoptilolite was reported by other authors [29]. The exo-peak at 1340 °C is probably due to a reaction of the melt with the corundum crucible.

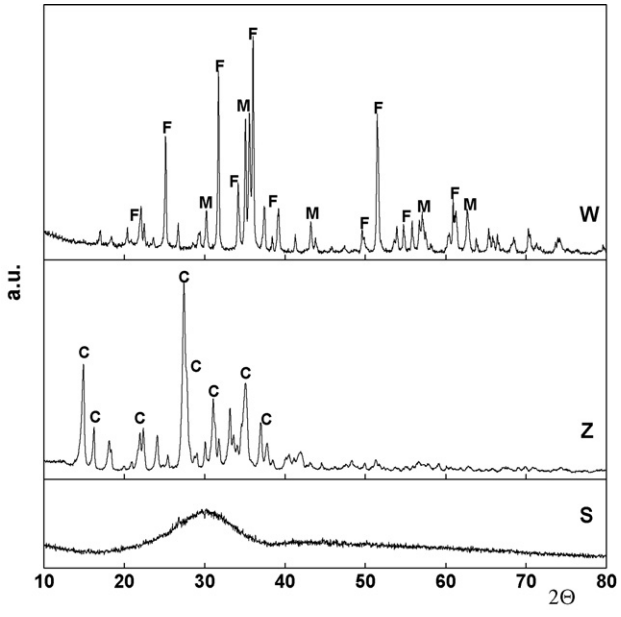

Fig. 1. XRD spectra of flotation waste (W), blast furnace slag (S) and zeolite tuff (Z). M, magnetite; F, fayalite; C, clinoptilolite.

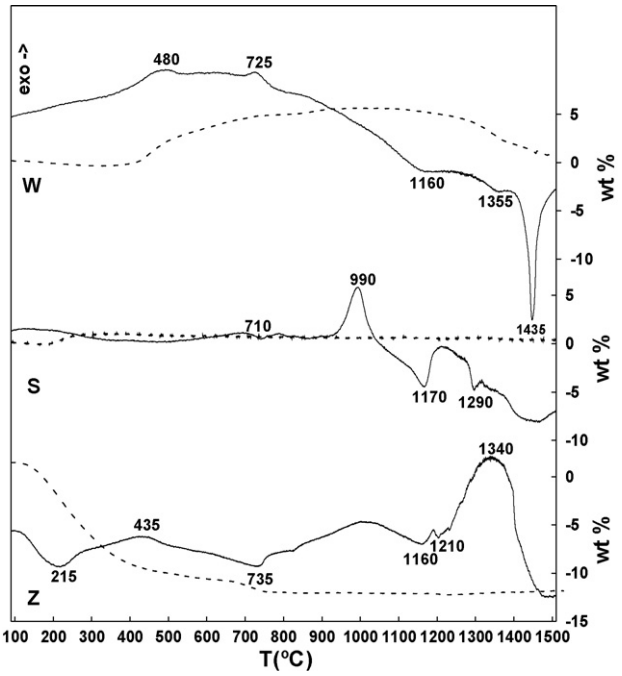

Fig. 2. TG–DTG traces of flotation waste (W), blast furnace slag (S) and zeolite tuff (Z).

The glass–ceramics obtained by mixing flotation waste with blast furnace slag would be characterized by a low SiO_2 and a high Fe_2O_3 and CaO contents, resulting in low chemical durability and uncontrolled crystallization. For this reason, two compositions based on three and four different raw materials were prepared: the first batch, labeled WSZ, was obtained by mixing 30% flotation waste, 30% blast furnace slag and 40% zeolite tuff; the second, labeled WG, was obtained by 30% copper flotation waste, 45% glass cullet, 15% quartz sand and 10% $CaCO_3$. The XRF analyses of the WSZ and WG glasses are reported in Table 1.

The batches were heated at 10 °C/min and melted for 30 min at 1400 °C. In both compositions no foaming was observed. The refining process was completed after only 10–15 min at 1400 °C, followed by formation of a smooth, mirror-like melt surface. The resulting glasses were free of visible bubbles. The short melting time at 1400 °C indicates a relatively low cost of the vitrification procedure.

The results of the TCLP test, carried out on the flotation waste, WSZ and WG glass frits are summarized in Table 2, together with the applied limits. The flotation stream itself must be characterized as an hazardous waste, while the glass frits show a very high chemical durability.

In previous studies with other iron-rich compositions it was demonstrated that the vitrification significantly reduces the

Table 2
TCLP results of the leached element concentrations (ppm)

	W	WSZ	WG	Applied limits
Zn	114.4 ± 1.2	0.14 ± 0.02	0.17 ± 0.02	0.5
Cu	94.9 ± 1.0	<0.005	0.008 ± 0.001	0.1
Pb	7.2 ± 0.4	0.0012 ± 0.0002	<0.001	0.2

leachability of the waste and that the transformation of the glasses in glass–ceramics additionally improves the chemical durability [14].

4.2. WSZ glass–ceramic

Fig. 3 presents the DTA (bold solid line), TG (dashed line) traces of WSZ powder sample, heat-treated in air and nitrogen and bulk sample in air. The TG trace of the powder sample in air shows about 0.5 wt% increasing due to Fe^{2+}oxidation after 650 °C. The maximum rate of oxidation, evaluated by the DTG peak (i.e. the TG derivate), is at 725 °C, which is in a good agreement with the exothermal effect at 710 °C. A large crystallization exothermal with low intensity occurs at 894 °C while the melting of the formed crystal phase occurs at 1166 °C.

In previous works it was shown that the surface oxidation reduces the magnetite ($FeO{\cdot}F_2O_3$) formation and the crystallization trend [11,12,15]. In reducing atmosphere or with a bulk sample no oxidation takes place and the crystallization rate is considerably higher. These results were confirmed in the present study by WSZ composition. The DTA and TG traces of the powder sample in nitrogen atmosphere and the bulk sample in air show no evident oxidation exo-effects and weight gains. At the same time, intensive crystallization peaks were observed at

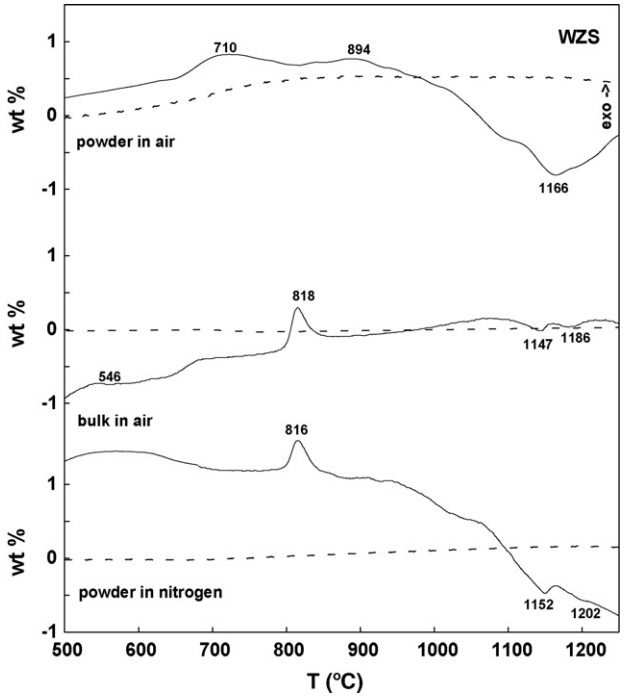

Fig. 3. TG–DTG of WSZ powder and bulk samples.

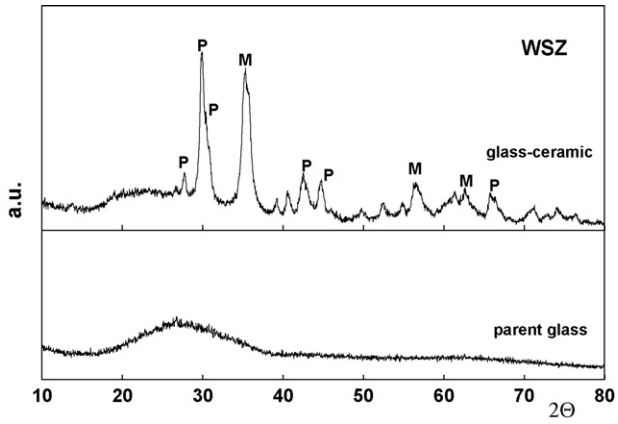

Fig. 4. XRD spectra of parent glass and final WSZ glass–ceramic. P, pyroxene and M, magnetite.

800–850 °C, followed by melting endo-effects at about 1150 and 1200 °C. The first and the second endo-effects are due to the melting of pyroxene and magnetite, respectively [11].

The predominance of bulk nucleation can be evaluated by the shift of the crystallization peak temperature, T_P, when bulk and powder samples are treated with the same thermal cycle: the smaller is the shift, bigger is the number of nuclei formed in the bulk [28]. For WZS glass, the T_P temperatures, occurr at 818 and 816 °C for the bulk in air and for the powder in N_2, respectively. The negligible difference indicates a spontaneous bulk nucleation yielding a fine crystalline glass–ceramic, obtained by one-step crystallization heat-treatment. This behavior, typical of iron-rich compositions, can be related to the liquid–liquid immiscibility at high temperature, where one of the liquid phases is richer in iron and promotes a spontaneous formation of the magnetite spinels. By prolonged thermal treatment the spinel crystals act as nuclei for the formation of the main pyroxene phase [9,15].

Bulk WZS samples (2 cm × 1 cm × 1 cm) were heated at 5 °C/min up to 800 °C, held for 1 and 5 h and cooled at 10 °C/min to room temperature. The XRD spectra of the parent glass and the glass–ceramic, obtained after 1 h holding, are presented in Fig. 4. The glass–ceramic spectrum corresponds to the formation

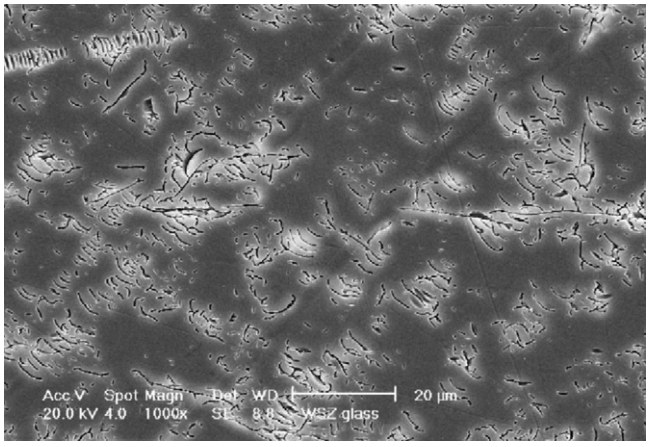

Fig. 5. SEM image of the parent WSZ glass.

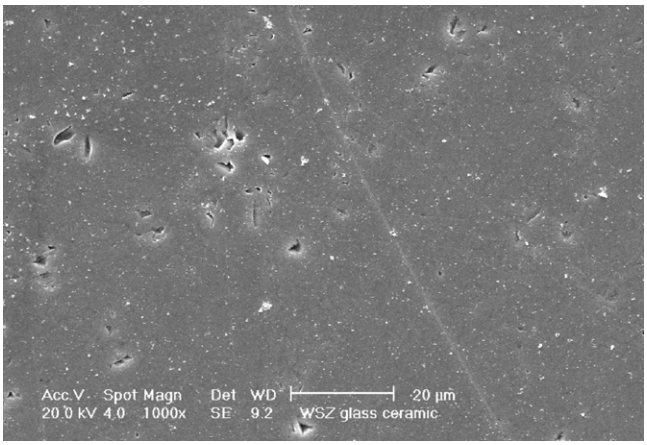

Fig. 6. SEM image of the final WSZ glass–ceramics.

of 20 ± 3 wt% magnetite spinel and 40 ± 3 wt% pyroxene solid solution. No significant variation was observed by prolonging the heat-treatment up to 5 h, highlighting that 1 h isothermal step at 800 °C is sufficient to complete the crystallization.

The morphology of the parent glass and the final glass–ceramic were observed by SEM. Fig. 5 shows an image of the non-homogeneous structure of the parent glass. Due to elevated atomic number of the iron and resulting higher electrons reflection, the iron-rich phase is presented by light spots with 3–6 μm size, randomly distributed in the matrix. It is well distinguished that these zones are also characterized by a lower chemical durability. Fig. 6 shows an image of the final glass–ceramic: in this case the structure is homogenous and with higher chemical resistance.

4.3. WG glass–ceramic

The DTA results of WG glass, shown in Fig. 7, indicate a low rate of crystallization. The powder sample in air shows an oxidation exo-effect in the range 750–850 °C, related to 0.35% weight gain in the TG trace, a low intensity exo-peak at 990 °C and an endo-effect at 1070 °C. The powder sample, heat-treated in nitrogen atmosphere, shows no oxidation, a exo-effect at 950 °C

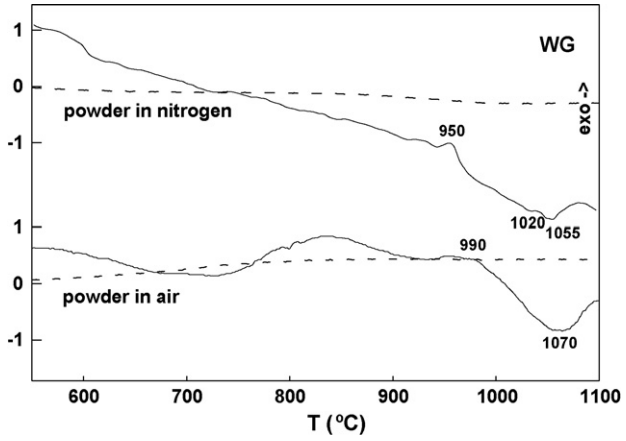

Fig. 7. DTG of WG powder samples in air and nitrogen atmosphere.

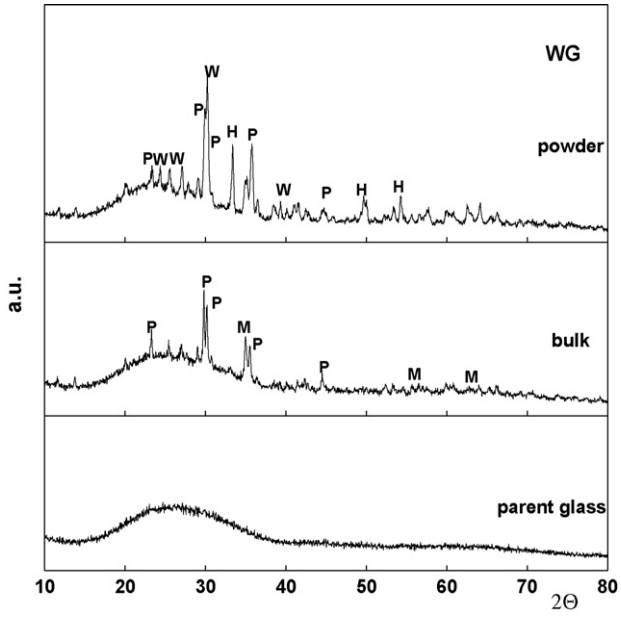

Fig. 8. XRD spectra of parent WG glass and powder and bulk samples, heat-treated at 1020 °C. P, pyroxene; W, wollastonite; M, magnetite; H, hematite.

and two low intensity melting peaks at 1020 and 1055 °C. No crystallization peak was observed in the DTA trace of the bulk sample.

Since iron-rich compositions with low crystallization rate are suitable to form sintered glass–ceramics [11,16], the WG frit was crushed and sieved to obtain two fractions: fine (below 0.5 mm), labeled F, and coarse (3–5 mm), labeled C. Using F fraction, placed loosely in a refractory mould, non-porous sintered samples with a smooth surface were obtained at 970–990 °C. The sintering of the C fraction was obtained at 1040–1060 °C. After grinding and polishing, the color the F and C sample were red-reddish brown and black, respectively.

The crystal phases, formed in F and C samples after 30 min sinter-crystallization at 1020 °C was determined by XRD and the spectra are shown in Fig. 8, together with the spectra of the parent glass. In F sample, wollastonite ($CaO{\cdot}SiO_2$) solid solution, pyroxene and hematite are formed, whereas in C—pyroxene and magnetite; the total crystallinity was estimated as 40 ± 3 and 25 ± 3%, respectively. The higher amount of crystal phase in F sample is due to the formation of wollastonite. This peculiarity may be related to the low MgO, MnO and Al_2O_3 percentages in the parent WG glass and to the iron oxidation process which reduces the total FeO amount and increases the CaO concentration in the surface layer [26].

An aesthetically appealing glass–ceramic was obtained by mixing 60 wt% F and 40% C fractions. The mix was placed loosely in a refractory form (10 cm × 10 cm) and heated in air at 20 °C/min up to 1020 °C, held 30 min and cooled at 10 °C/min. After grinding and polishing, the samples acquired a granite-like appearance. Due to the hematite (Fe_2O_3) formation on the surface, the color of the powders becomes red-brown, while the color of the coarse particles remained black, as the parent glass. Combining, in the proper proportion, fine and coarse glass

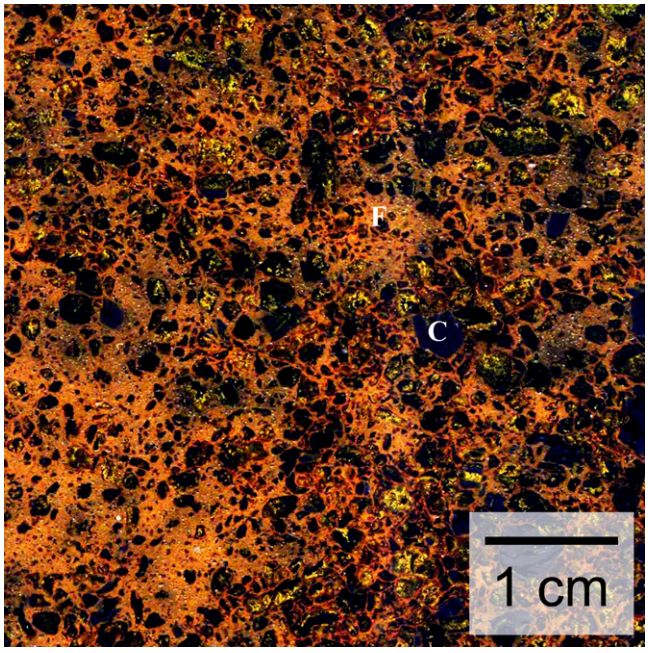

Fig. 9. WG sintered glass–ceramic (F, zone with fine particles and C, a coarse particle).

particles an attractive chromatic effect, shown in Fig. 9, was obtained after sintering, grinding and polishing.

Fig. 10 is an optical microscopy image of WG glass–ceramic, where the superficial hematite layer (labeled H) and the large pyroxene crystals (labeled P), formed in the bulk of the coarse particles can be easily distinguished.

The mechanical properties of sintered iron-rich glass–ceramics by other hazardous industrial wastes were reported in previous works. Bending strength of 80–120 MPa and Young's modulus of 70–80 GPa were measured for samples by press powders [16], while bending strength of 70–80 MPa and Young's modulus of 50–60 GPa—for materials by frit sintering [30]. These characteristics significantly surpass the values of the traditional (ceramics) and natural (marbles and granites) building tiling materials.

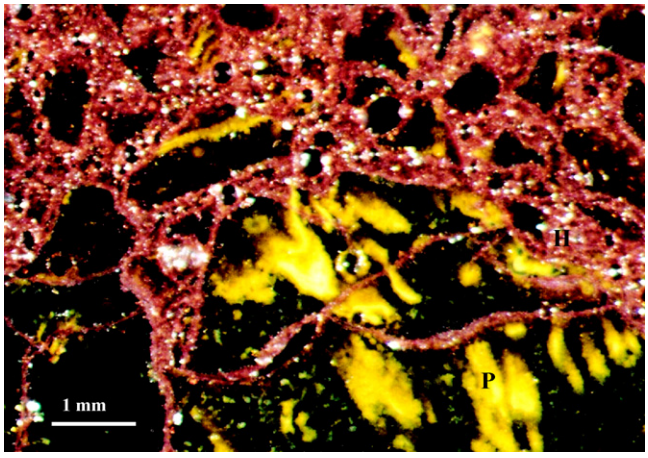

Fig. 10. Optical microscopy images of WG sintered glass–ceramic.

5. Conclusions

Two iron-rich glass compositions showing a high chemical durability were obtained by mixing a flotation waste from copper production with blast furnace slag and raw materials.

The first glass was characterized by a spontaneous liquid–liquid separation and a high crystallization rate. It was transformed into a glass–ceramic material with 60% crystal phase by 1 h heat-treatment at 800 °C.

The second glass showed a low crystallization rate and good sinterability. By mixing fine and coarse grain fractions followed by sinter-crystallization at 1020 °C, glass–ceramics with an appealing granite-like appearance were obtained.

Acknowledgments

The authors express thanks to Dr. Semra Çoruh for the waste samples and the information about their origin and to Dr. Giuliana Taglieri for the XRD analysis.

References

[1] B. Locsei, Molten Silicates and their Properties, Akademiai Kiado, Budapest, 1970.
[2] H. Beall, H.L. Rittler, Basalt glass ceramics, Ceram. Bull. 55 (1976) 579–582.
[3] S.A. Morse, Basalts and Phase Diagrams, Springer-Verlag, New York, 1982.
[4] J. Hlavac, The Technology of Glass and Ceramics: An Introduction, Elsevier, Amsterdam, 1983.
[5] D.F. Bickford, C.M. Jantzen, Devitrification of defense nuclear waste, glass: role of melt insolubles, J. Non-Cryst. Solids 84 (1986) 299–307.
[6] D. Schreiber, B.K. Kochanowski, C.W. Shreberg, Compositional effect on the iron redox state in model glasses for nuclear waste immobilization, ceramic transactions, in: G.B. Mellinger (Ed.), Environmental and Waste Management Issues in the Ceramic Industry, vol. 39, The American Ceramic Society, 1994, pp. 141–150.
[7] I.W. Donald, B.L. Metcalfe, R.N. Taylor, Review—the immobilization of high level radioactive wastes using ceramics and glasses, J. Mater. Sci. 32 (1997) 5851–5887.
[8] M. Pelino, C. Cantalini, J.Ma. Rincon, Preparation and properties of glass–ceramic materials obtained by recycling goethite industrial waste, J. Mater. Sci. 32 (1997) 4655–4660.
[9] M. Romero, J.Ma. Rincon, Preparation and properties of high iron content glasses obtained from industrial wastes, J. Eur. Ceram. Soc. 18 (1998) 153–160.
[10] M. Romero, J.Ma. Rincon, Surface and bulk crystallization of glass–ceramics in the Na_2O–CaO–ZnO–PbO–Fe_2O_3 system derived from a goethite waste, J. Am. Ceram. Soc. 82 (1999) 1313–1317.
[11] A. Karamanov, G. Taglieri, M. Pelino, Iron-rich sintered glass–ceramics from industrial wastes, J. Am. Ceram. Soc. 82 (1999) 3012–3016.
[12] A. Karamanov, P. Pisciella, M. Pelino, The crystallisation kinetics of iron rich glasses in different atmospheres, J. Eur. Ceram. Soc. 20 (2000) 2233–2237.
[13] A. Karamanov, P. Pisciella, C. Cantalini, M. Pelino, Influence of the Fe^{3+}/Fe^{2+} ratio on the crystallization of iron-rich glasses made with industrial wastes, J. Am. Ceram. Soc. 81 (2000) 3153–3157.
[14] P. Pisciella, S. Crisucci, A. Karamanov, M. Pelino, Chemical durability of glasses obtained by vitrification of industrial wastes, Waste Manage. 21 (2001) 1–9.
[15] A. Karamanov, M. Pelino, Crystallization phenomena in iron rich glasses, J. Non-Cryst. Solids 281 (2001) 139–151.
[16] A. Karamanov, G. Taglieri, M. Pelino, Sintering in nitrogen atmosphere of iron-rich glass–ceramics, J. Am. Ceram. Soc. 87 (2004) 1354–1357.

[17] J. Aota, L. Morin, S. Mikhail, T. Chen, D. Liang, Immobilization of hazardous elements in EAF dust by vitrification process, Waste Process. Recycl. 5 (1995) 335–349.
[18] B.E. Roger, J.E. Schlobohm, Glassification of electric arc furnace dust, Iron Steel Eng. 4 (1993) 23–26.
[19] M. Pelino, A. Karamanov, P. Pisciella, D. Zanneti, S. Crisucci, Vitrification of electric arc furnace dusts, Waste Manage. 22 (2002) 945–949.
[20] T.W. Cheng, Combined glassifcation of EAF dust and incinerator fly ash, Chemosphere 50 (2003) 47–51.
[21] E. Kuleva, L. Orlova, O. Borisov, M. Gulikin, Glass–ceramics on base of iron containing industrial wastes, in: Proceedings of the XVIIIth ICG, San Francisco, USA, Am. Ceram. Soc. (1998).
[22] E.B. Ferreira, E.D. Zanotto, L.A.M. Scudeller, Glass and glass–ceramic from basic oxygen furnace (BOF) slag, Glass Technol. 75 (2002) 75–86.
[23] A.A. Francis, R.D. Rawlings, R. Sweeney, Crystallization kinetic of glass particles prepared from a mixture of coal ash and soda-lime cullet glass, J. Non-Cryst. Solids 333 (2004) 187–193.
[24] P. Kavouras, Ph. Komninou, K. Chrissafis, G. Kaimakamis, S. Kokkou, K. Paraskevopoulos, Th. Karakostas, Microstructural changes of processed vitrified solid waste products, J. Eur. Ceram. Soc. 23 (2003) 1305–1311.
[25] Th. Kehagias, Ph. Komninou, P. Kavouras, K. Chrissafis, G. Nouet, Th. Karakostas, Crystal phase separation and microstructure of a thermally treated vitrified solid waste, J. Eur. Ceram. Soc. 26 (2006) 1141–1148.
[26] R.D. Cooper, J.B. Fanselow, D.B. Poker, The mechanism of oxidation of a basaltic glass: chemical diffusion of network-modifying cations, Geochim. Cosmochim. Acta 60 (1996) 3253–3265.
[27] D.J.M. Burkhard, T. Scherer, Surface oxidation of basalt glass/liquid, J. Non-Cryst. Solids 352 (2006) 241–247.
[28] Z. Strnad, Glass–Ceramic Materials, Elsevier, Amsterdam, 1986.
[29] V. Pérez Moreno, J.J. Castro Arellano, H. Balmori Ramirez, Characterization and preparation of porous membranes with a natural Mexican zeolite, J. Phys.: Condens. Matter 16 (2004) S2345–S2352.
[30] A. Karamanov, M. Pelino, Granite-like tilling sintered glass–ceramics from industrial wastes, in: Proceedings of the Sustainable Waste Management and Recycling: Challenges and Opportunities, London, 2004, pp. 225–239.